Silver Nanodesert Rose as a Substrate for Surface-Enhanced Raman Spectroscopy

Albert Gutes,[†] Carlo Carraro,[‡] and Roya Maboudian*

Department of Chemical Engineering, University of California, Berkeley, California 94720

ABSTRACT Silver galvanic displacement on silicon has been employed to produce large-area reproducible substrates, with morphology similar to that of the natural desert rose but on the micrometer scale. The process is based on an extremely simple wet chemistry approach using only AgF and KF, as silver and fluoride sources. A key element is the absence of HF in the deposition solution, which has been commonly used in previous silver galvanic displacement processes. The new process affords a higher degree of control in the redox reaction than those reported previously. The structures formed in this manner possess a large area-to-volume ratio with a high density of rough silver flakes uniformly distributed across the substrate. The silver morphology on the nanometer scale is shown to provide an excellent platform for surface-enhanced Raman spectroscopy (SERS), yielding detection levels for *trans*-1,2-bis(4-pyridyl)ethylene, 4-mercaptopyridine, and Rhodamine 6G in solution down to ppb, ppt, and ppq limits, respectively. The SERS reproducibility on the substrate was verified by monitoring the signal intensity variations across the sample. The simplicity of the substrate fabrication process, as well as the excellent uniformity, opens up opportunities for the quantitative and in-field chemical trace analysis using these substrates.

KEYWORDS: silver • galvanic displacement • SERS • BPE • 4-Mpy • Rhodamine 6G

1. INTRODUCTION

Since the discovery of the surface-enhanced Raman spectroscopy (SERS) effect in 1974 by Fleischman et al. (1), significant effort has been directed toward the fabrication of substrates that provide high enhancement factors (EFs) in a reproducible manner (2−4). The SERS effect is attributed to the strong light-induced electric field at specific sites, coined "hot spots", where the Raman signal can be magnified up to a theoretical value of 10^{14}, permitting the detection of single molecules (5). The presence or absence of hot spots is related to the morphology of the substrate at the nano- and micrometer levels, with various schemes being explored for the fabrication of SERS-active substrates. Examples include nanofilms (6), nanoparticles (7), nanowires (8), and nanorods (9). One of the ongoing challenges is the difficulty in the reproducible fabrication of substrates containing a high density of hot spots that could provide tools for the large-scale realization of SERS-based sensors for chemical, biological, or medical analyses (10−13).

Here we present the use of a simple method, based on controlled silver galvanic displacement on silicon, to produce substrates that show promising results for use in quantitative SERS analysis. Our method is based on the use of electroless deposition through a galvanic displacement process in which silver is reduced in a controlled manner on a silicon surface, which acts as the reducing agent. Previous efforts that combine electroless deposition of silver (using a different plating solution than the one we present here) with SERS analysis have been published (14, 15). The difference between the present work and the two earlier publications is that the first one uses random uncontrolled formation of silver dendrites on silicon that are poorly adhered to the surface (14), while the second one is based on the decoration of silicon nanowires grown via a vapor−liquid−solid mechanism (15). The main drawback in both cases is the lower reproducibility in the fabrication process compared to the process we present here. Depending on the relative amounts of the various reactants, the redox reaction leads to different final structures, ranging from smooth thin films to nanostructured films, including one termed nanodesert rose, which is presented here because of its extreme usefulness for SERS analysis. Because of the random organization of the silver nanoflakes produced by this method, hot spots are distributed uniformly over the entire surface, junctions, and facets and are easily found by a simple focusing, using an optical microscope, before SERS measurement. Because of the random distribution and roughness of the silver flakes, we have investigated and found that any point on the sample surface presents the same SERS activity and thus any spot can be considered as a hot spot. This feature simplifies enormously the tedious process of location and focusing prior to SERS analysis.

SERS activities of the substrates are tested by immersion in solution using three organic molecules, *trans*-1,2-bis(4-pyridyl)ethylene (BPE), 4-mercaptopyridine (4-MPy), and Rhodamine 6G (R6G). In all cases, high-quality Raman spectra were obtained down to the ppb, ppt, and ppq concentration levels, respectively. The latter molecule, R6G, is often employed in SERS studies, owing to its large Raman cross section, while the former two offer the chance to compare the signals from identical moieties (4-pyridyl rings)

* Tel.: +1 (510) 643-3489. Fax: +1 (510) 642-4778. E-mail: maboudia@berkeley.edu.

Received for review July 15, 2009 and accepted October 5, 2009

† E-mail: agutes@gmail.com.

‡ E-mail: carraro@yahoo.com.

DOI: 10.1021/am9004754

with different end groups (mercapto vs 4-pyridyl) that possess rather different chemical interactions with the silver substrate. The vast differences observed in the detection limits (and EFs) underline the importance of both the orientation of the molecules on the substrates and the chemical enhancement mechanisms in SERS.

2. EXPERIMENTAL SECTION

Chemicals. All chemicals were ACS grade. AgF (99.9%) and KF (99+%) were used for the preparation of the galvanic displacement plating solution (Sigma-Aldrich Co. Ltd.). *trans*-1,2-Bis(4-pyridyl)ethylene (BPE; recrystallized from 97%), 4-mercaptopyridine (4-MPy; 95%), and Rhodamine 6G (R6G; 99%) were used as SERS analytes (Sigma-Aldrich Co. Ltd.). Double-distilled water (resistivity of 18 MΩ) was used throughout except for the preparation of BPE and 4-MPy dissolutions, where methanol (EMB) was used as the solvent.

SERS Substrate Fabrication. To synthesize the SERS substrate, silicon ⟨111⟩ chips, 5 × 5 mm in size, were degreased by sonication in acetone and isopropyl alcohol for 10 min and then rinsed with deionized (DI) water before drying in gentle N_2. A native oxide layer was removed by immersing the chips in concentrated HF for 1 min, rinsed in DI water, and dried in N_2. A silver plating solution for the galvanic displacement process was prepared by dissolving the appropriate amounts of AgF and KF in DI water to a final Ag^+ concentration of 30 mM and a F^- concentration of 600 mM. Silicon chips were immersed immediately after native oxide etching, left in solution for 24 h, then rinsed in DI water, and dried with N_2. The electroless galvanic displacement process leads to the formation of pure interconnected silver rough flakes, with an approximate area of 20 μm^2 and a thickness of 200 nm per flake.

SERS Measurements. Silver nanostructures were immersed in the less concentrated solution of each analyte, measured while in solution, rinsed in methanol (when measuring BPE or 4MPy) or water (R6G measurements), and dried before immersion in the consecutively more concentrated solution. Raman measurements (Horiba Jobin Yvon LabRAM) were performed in a backscattering configuration with an excitation line provided by a He−Ne laser (632.8 nm wavelength, 10 mW at the sample) through an Olympus BX41 confocal microscope (100× objective; numerical aperture = 0.8). Each Raman spectrum was the result of averaging 10 scans with 10 s integration time in the 920−1800 cm^{-1} region. SERS hot-spot uniformity was examined by monitoring the signal uniformity from a full monolayer of 4-MPy. This method was preferred to the solution measurement, in order to avoid potential measurement bias due to the higher coverage on the spots probed at later times. A monolayer coverage obviously yields signals much above the detection limit, but every point on the surface is treated equally because for thiol species one monolayer is the saturation coverage. A monolayer of 4-MPy was prepared by 24 h of incubation of a fresh desert rose substrate. After incubation, rinsing in methanol was performed to remove the adsorbed molecules on the surface followed by drying in a gentle N_2 flow. Six random points across the substrate were measured, with each spectrum consisting of 10 scans with 3 s of integration time recorded. The reproducibility is calculated as the percent deviation in the 1013 cm^{-1} peak intensity.

3. RESULTS AND DISCUSSION

Figure 1 is a scanning electron microscopy (SEM; NovelX) image of the final structure, which consists of interconnected rough silver flakes that resemble the natural desert rose. X-ray photoelectron spectroscopy (XPS) analysis (Omicron) confirmed the metallic silver nature of the formed structures.

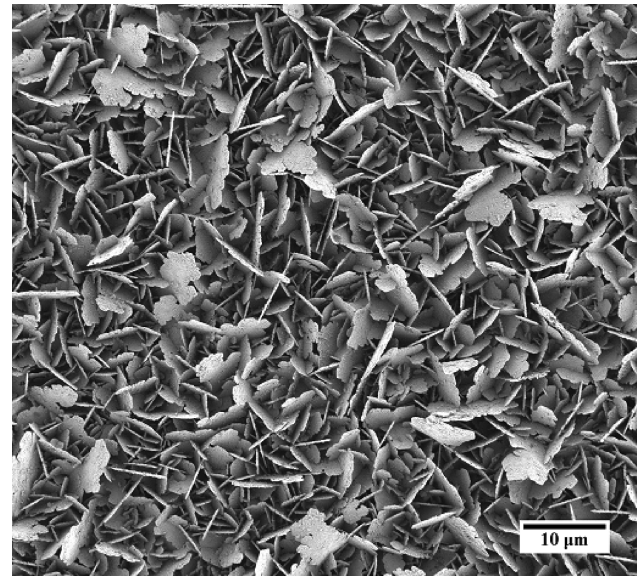

FIGURE 1. SEM image of the presented silver "desert rose" on silicon. The plating solution contained 30 mM Ag^+ and 600 mM F^- ions. The immersion time was 24 h.

The large surface area-to-volume ratio provides a promising candidate for a reproducible SERS substrate with high EFs. Complete and uniform coverage of the surface is achieved by this preparation method, suggesting this as a promising approach for large-scale production. Hot spots can be found by optical microscopy by focusing on any of the flake sheets without any other precautions.

Figure 2A shows the obtained Raman spectra when BPE solutions with different concentrations (10^{-7} M up to 10^{-4} M, or 18 ppb to 18 ppm) were tested. The characteristic ring breathing mode at around 1000 cm^{-1} and the ring deformation mode at around 1600 cm^{-1} as well as the 1200 cm^{-1} peak were used as identifiers for the BPE molecule (16−18). 10^{-8} M BPE did not show any characteristic peaks, and thus the 10^{-7} M concentration is taken as the limit of detection for the BPE molecule. Figure 2B compares the Raman spectra of a 10^{-2}M BPE solution obtained when using the desert rose (a) and a 50 nm evaporated silver on a silicon chip (b) acting as a non-SERS substrate. Even though the silver film on the surface provides some enhancement because of the intrinsic silver SERS capacity in the measurements, the total absence of Raman signals when using other non-SERS substrates (bare silicon or aluminum film) forced us to use silver thin films in order to be able to compare the SERS substrate enhancement to some extent.

This high concentration was necessary in order to be able to directly compare the SERS-active substrate with a non-SERS substrate because the flat 50 nm silver surface did not show any Raman signal when the BPE concentration was lower than 10^{-2} M. By direct comparison of the last two spectra, it is possible to demonstrate the large enhancement due to the desert rose substrate. Because many definitions can be found in the literature for the SERS EF (19, 20), we calculate the EF by using the analytical chemistry point of view through the analytical EF (AEF) defined as (19)

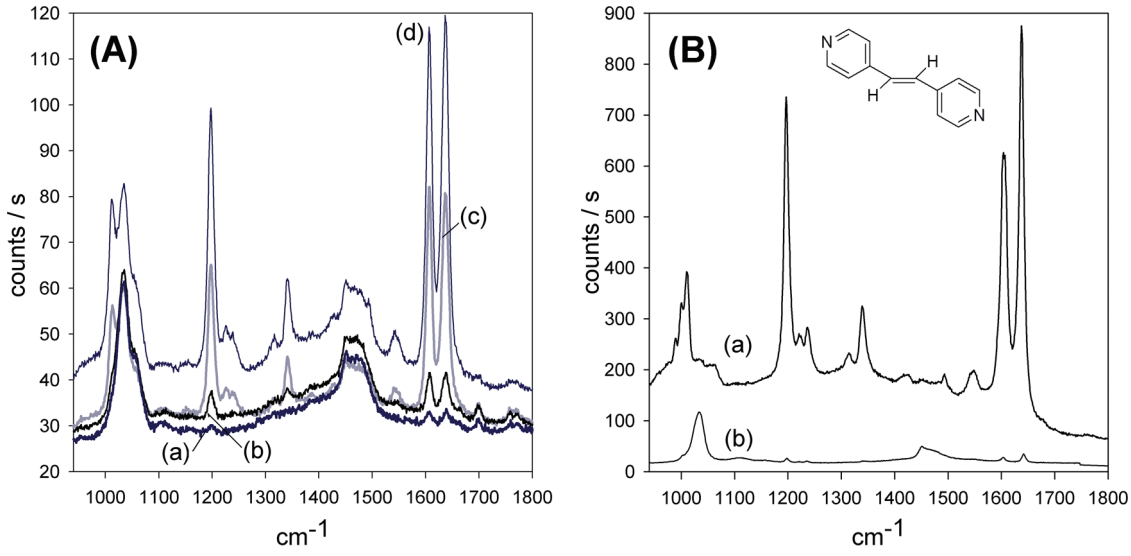

FIGURE 2. Raman spectra obtained using the BPE molecule. (A) Spectra measured while a silver nanostructure was immersed in a solution with BPE concentrations of (a) 10^{-7} M, (b) 10^{-6} M, (c) 10^{-5} M, and (d) 10^{-4} M. (B) Comparison of spectra obtained in a 10^{-2} M solution using (a) SERS-active silver nanostructures and (b) a non-SERS 50 nm evaporated silver substrate. The BPE structure is shown as the inset in part B.

$$\mathrm{AEF} = (I_{\mathrm{SERS}}/C_{\mathrm{SERS}})/(I_{\mathrm{RS}}/C_{\mathrm{RS}})$$

where I_{SERS} corresponds to the Raman intensity obtained for the SERS substrate under a certain concentration C_{SERS} and I_{RS} corresponds to the Raman intensity obtained under non-SERS conditions at an analyte concentration of C_{RS}, taking into account that the experimental conditions, such as the laser wavelength, laser power, microscope objective or lenses, spectrometer, and measuring conditions on the substrate, are identical in all cases.

According to this established definition, we can obtain a value of AEF = 3×10^4 when using $C_{\mathrm{SERS}} = 10^{-7}$ M and $C_{\mathrm{RS}} = 10^{-2}$M and the intensities obtained from parts A and B of Figure 2, respectively. XPS analysis showed a planar orientation of the BPE molecules in relation to the surface.

Figure 3A shows the spectra obtained when the desert rose substrate was immersed in 4-MPy solutions of different concentrations, following the same procedure from low to high concentration as that in the BPE measurements. Characteristic 4-MPy peaks were found at 1013, 1050, and 1100 cm^{-1} for the in-plane deformations and trigonal ring breathing with C═S as well. Peaks around 1550 cm^{-1}, typical for the 4-MPy molecule, are also found as described in Table 1 of the Wang and Rothberg results (21). In this case, a concentration of 10^{-10} M was able to be detected, as shown in spectrum c of Figure 3A. A lower concentration of 10^{-11}

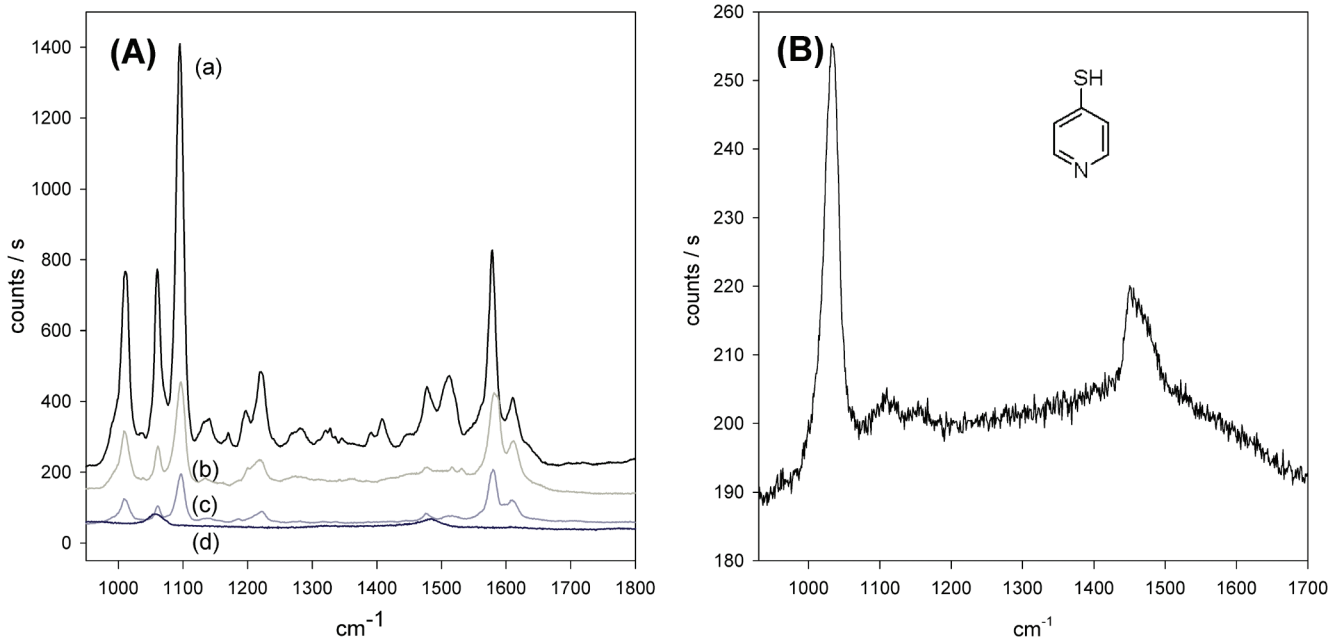

FIGURE 3. (A) Raman spectrum of different concentrations of 4-MPy on the desert rose sample: (a) 10^{-6} M; (b) 10^{-8} M; (c) 10^{-10} M; (d) 10^{-11} M. The 4-MPy structure is also shown in the figure. (B) Raman spectrum of a 10^{-2} M 4-MPy solution when measured using a non-SERS 50 nm evaporated silver as the substrate.

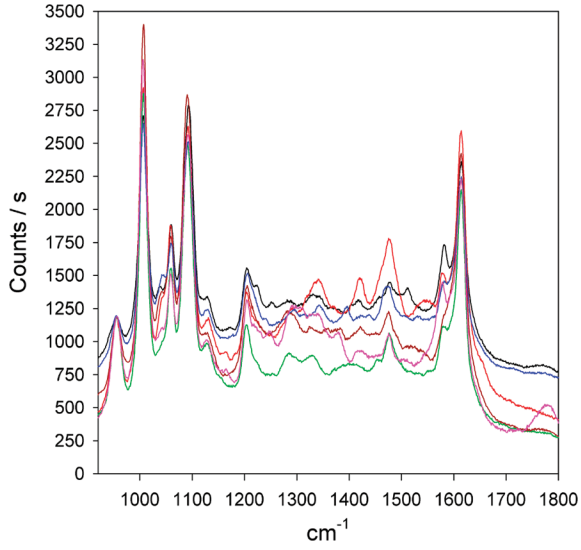

FIGURE 4. Raw data for the substrate reproducibility test. Six random points were measured after the formation of a 4-MPy SAM. The reproducibility is expressed as the deviation in the 1013 cm^{-1} peak intensity and is found to be lower than 15%.

M (part d of Figure 3A) did not present any of the characteristic peaks of 4-MPy. In this case, it was possible to detect a 10^3 times lower concentration when compared with BPE spectra. It is suggested that 4-MPy chemically interacts with the silver substrate via the S—Ag bond, in contrast to a weaker interaction between the BPE molecule and the silver substrate. This difference may be responsible for the observed differences in the EFs for these two molecules.

Figure 3B shows the Raman signal obtained when a 50 nm evaporated silver on silicon was immersed and measured in a 10^{-2} M 4-MPy solution. It is clearly shown that peaks are not clearly defined, and the signal intensity for the 1013 cm^{-1} peak is extremely weak when compared to the ones using the desert rose substrate with much lower concentrations. When using this concentration as C_{RS} and a concentration of 10^{-6} M as C_{SERS} and using the obtained intensities shown in Figure 3, it is possible to establish a value of AEF = 2×10^5 when using 4-MPy as the analyte. Compared to the AEF value obtained on BPE, it can be pointed out that the amount of molecules present on the 4-MPy SERS is larger because of the different molecular orientations. While BPE lies planar on the surface, 4-MPy can form vertical self-assembled monolayers (SAMs) because of the thiol—silver interaction. We believe that this increase in the number of molecules can be the reason for the higher SERS signal observed with 4-MPy.

Figure 4 shows the reproducibility test performed on a silver desert rose sample after 4-MPy monolayer incubation and rinsing. Six random points, separated by millimeter distances, were measured. As can be observed, very good reproducibility is achieved in the characteristic peaks of 4-MPy at 1013, 1050, 1100, and 1600 cm^{-1}. The peak height at 1013 cm^{-1} was treated statistically after appropriate background subtraction for each spectrum. The results show a mean value of the peak height of 2128 ± 300 counts/s (95% confidence level), which is equivalent to a 14% deviation.

Figure 5A shows the spectra obtained when the desert rose substrate was used while immersed in R6G solutions down to the 10^{-15}M (ppq) concentration limit. This is the first time that R6G is reported to be detected at the ppq level in a reproducible way. Recent literature reports detection limits of 10^{-8} M (22), 10^{-9} M (23, 24), and 10^{-12} M (25). Part B in this figure shows the non-SERS activity of a 50 nm evaporated silver when immersed in a 10^{-3} M R6G solution. In this case, using again the established definition of AEF, C_{RS} of 10^{-3} M, and C_{SERS} of 10^{-13} M, the final value of AEF is equal to 2×10^{10}.

4. CONCLUSIONS

In conclusion, an efficient, simple, reproducible, and versatile SERS substrate based on controlled silver galvanic displacement on silicon has been presented. Simplicity in

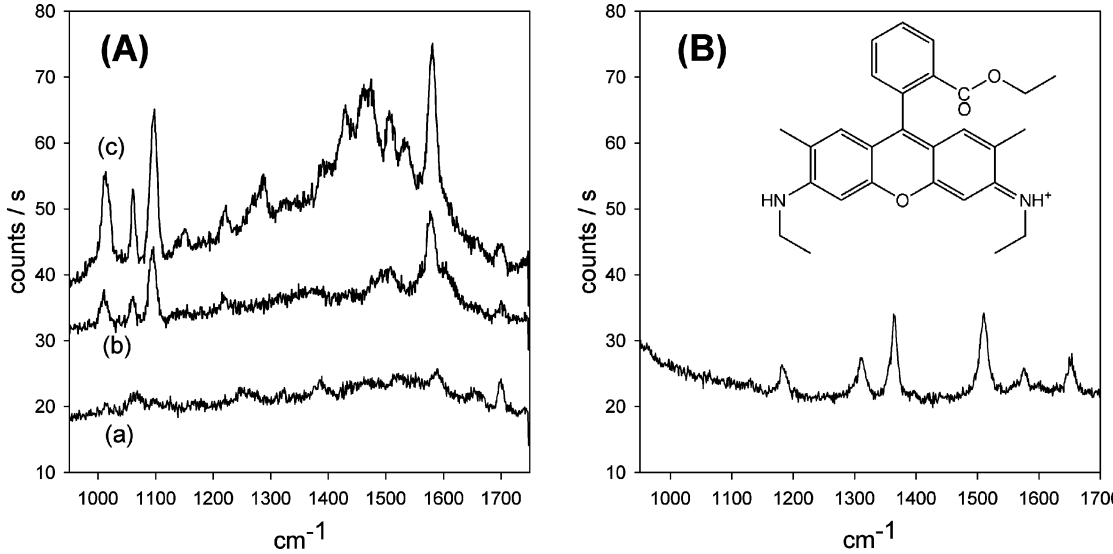

FIGURE 5. Raman spectra obtained using the R6G molecule. (A) Spectra measured while a silver nanostructure was immersed in solution with R6G concentrations of (a) 10^{-15} M, (b) 10^{-14} M, and (c) 10^{-13} M. (B) Raman spectrum of a 10^{-3} M R6G solution when measured using a non-SERS 50 nm evaporated silver as the substrate.

the production of the silver structures compared to expensive lithographic methodologies combined with the high Raman EFs obtained provide an exceptionally cost-effective, with a reproducible fabrication method, substrate for SERS analysis. Three different target molecules were examined to determine the SERS activity of the presented substrate. A BPE concentration of 10^{-7} M (18 ppb) was clearly detected, a concentration of 10^{-10} M (11 ppt) was detectable when using 4-MPyr as the analyte, and finally 10^{-15} M (0.5 ppq) was clearly detected for R6G. The large differences in the detection limits highlight the importance of physical and chemical interactions of the analytes with the substrates, as well as the enhancement provided by the molecular orientation of the substrate. Final EFs can be estimated as 3×10^4 for BPE, 2×10^5 for 4-MPy, and 2×10^{10} for R6G when compared to evaporated flat silver substrates.

Acknowledgment. This work was funded by the DARPA SERS S&T Fundamental Program under LLNL Subcontract B573237. A.G. thanks the Comissionat per a Universitats i Recerca (CUR) del Departament d'Innovació, Universitat i Empresa de la Generalitat de Catalunya for funding through the Beatriu de Pinós postdoctoral program.

REFERENCES AND NOTES

(1) Fleischman, M.; Hendra, P. J.; McQuilla, A. J. *Chem. Phys. Lett.* **1974**, *26*, 163–166.
(2) Moskovits, M. *Rev. Mod. Phys.* **1985**, *57*, 783–826.
(3) Campion, A.; Kambhampati, P. *Chem. Soc. Rev.* **1998**, *27*, 241–250.
(4) Kneipp, K.; Kneipp, H.; Kneipp, J. *Acc. Chem. Res.* **2006**, *39*, 443–450.
(5) Dieringer, J. A.; Wustholz, K. L.; Masiello, D. J.; Camden, J. P.; Kleinman, S. L.; Schatz, G. C.; Van Duyne, R. P. *J. Am. Chem. Soc.* **2009**, *131*, 849–854.
(6) Dick, L. A.; McFarland, A. D.; Haynes, C. L.; Van Duyne, R. P. *J. Phys. Chem. B* **2002**, *106*, 853–860.
(7) Wang, C. H.; Sun, D. C.; Xia, X. H. *Nanotechnology* **2006**, *17*, 651–657.
(8) Yoon, I.; Kang, T.; Choi, W.; Kim, J.; Yoo, Y.; Joo, S. W.; Park, Q. H.; Ihee, H.; Kim, B. *J. Am. Chem. Soc.* **2009**, *131*, 758–762.
(9) Guo, S. J.; Dong, S. J.; Wang, E. K. *Cryst. Growth Des.* **2009**, *9*, 372–377.
(10) Das, G.; Mecarini, F.; Gentile, F.; De Angelis, F.; Kumar, H. G. M.; Candelero, P.; Liberale, C.; Cuda, G.; Di Fabricio, E. *Biosens. Bioelectron.* **2009**, *24*, 1693–1699.
(11) Mahajan, S.; Richardson, J.; Brown, T.; Bartlett, P. N. *J. Am. Chem. Soc.* **2008**, *130*, 15589–15601.
(12) Shanmukh, S.; Jones, L.; Driskell, J.; Zhao, Y. P.; Dluhy, R.; Tripp, R. A. *Nano Lett.* **2006**, *6*, 2630–2636.
(13) Haes, A. J.; Chang, L.; Klein, W. L.; Van Duyne, R. P. *J. Am. Chem. Soc.* **2005**, *127*, 2264–2271.
(14) Lin, H. H.; Mock, J.; Smith, D.; Gao, T.; Sailor, M. J. *J. Phys. Chem. B* **2004**, *108*, 11654–11659.
(15) Galopin, E.; Barbillat, J.; Coffinier, Y.; Szunerits, S.; Patriarche, G.; Boukherroub, R. *ACS Appl. Mater. Interfaces* **2009**, *1*, 1396–1403.
(16) Seney, C. S.; Gutzman, B. M.; Goddard, R. H. *J. Phys. Chem. C* **2009**, *113*, 74–80.
(17) Khan, M. A.; Hogan, T. P.; Shanker, B. *J. Raman Spectrosc.* **2008**, *39*, 893–900.
(18) Freeman, R. G.; Hommer, M. B.; Grabar, K. C.; Jackson, M. A.; Natan, M. J. *J. Phys. Chem.* **1996**, *100*, 718–724.
(19) Le Ru, E. C.; Blackie, E.; Meyer, M.; Etchegoin, P. G. *J. Phys. Chem. C* **2007**, *111*, 13794–13803.
(20) Natan, M. J. *Faraday Discuss.* **2006**, *132*, 321–328.
(21) Wang, Z.; Rothberg, L. J. *J. Phys. Chem. B* **2005**, *109*, 3387–3391.
(22) Qiu, T.; Wu, X. L.; Shen, J. C.; Chu, P. K. *Appl. Phys. Lett.* **2006**, *89*, 131914.
(23) Chen, H. J.; Wang, Y. L.; Qu, J. Y.; Dong, S. J. *J. Raman Spectrosc.* **2007**, *38*, 1444–1448.
(24) Sakano, T.; Tanaka, Y.; Nishimura, R.; Nedyalkov, N. N.; Atanasov, P. A.; Saiki, T.; Obara, M. *J. Phys. D: Appl. Phys.* **2008**, *41*, 235304.
(25) Duan, G. T.; Cai, W. P.; Luo, Y. Y.; Li, Z. G.; Li, Y. *Appl. Phys. Lett.* **2006**, *89*, 211905.

AM9004754